DOI: 10.1021/ma100688n

Macromolecules
ARTICLE

Tailoring Polylactide Degradation: Copolymerization of a Carbohydrate Lactone and *S,S*-Lactide

Min Tang,[†,‡] Yixiang Dong,[‡] Molly M. Stevens,[‡] and Charlotte K. Williams*[,†]

[†]*Department of Chemistry, Imperial College London, London, United Kingdom SW7 2AZ, and*
[‡]*Department of Materials and Institute for Biomedical Engineering, Imperial College London, London, United Kingdom SW7 2AZ*

Received March 30, 2010; Revised Manuscript Received July 28, 2010

ABSTRACT: A series of copolymers are reported, synthesized via the random copolymerization of acetic acid 5-acetoxy-6-oxotetrahydropyran-2-yl methyl ester (**1**), and *S,S*-lactide. The copolymers are characterized by ^{1}H NMR spectroscopy, size exclusion chromatography (SEC), differential scanning calorimetry (DSC), thermal gravimetric analysis (TGA), and static water contact angle measurements. Four different copolymer compositions are obtained with 1 (RP1), 6 (RP2), 11 (RP3), and 25 wt % (RP4) of ring-opened monomer **1** incorporated with ring-opened *S,S*-lactide, and these are compared with a sample of poly(*S,S*-lactide) (P-*S,S*-LA) of related number-averaged molecular weight. As the loading of ring-opened monomer **1** increases, the glass transition temperatures of the copolymers decrease, in line with the values calculated using the Fox equation. The glass transition temperatures can, therefore, be controlled within the range 55 °C (RP1)−46 °C (RP4). The copolymers are spin-coated onto glass or electrospun into fibers and the static water contact angles determined. The static water contact angles, measured for either the fibers or the films, depend on the loading of ring-opened monomer **1** in the copolymers. The contact angle for RP4 is ∼7° lower than that of P-*S,S*-LA. The degradation of the copolymers is studied using size exclusion chromatography (SEC) conducted using samples in phosphate buffered chloroform solutions, enabling determination of the degradation rate constant. The degradation experiments show that as the loading of ring-opened monomer **1** in the copolymers increases, the degradation rate constants increase; thus, RP4 degrades ∼4 times faster than P-*S,S*-LA or RP1. Electrospun fibers of the copolymers are used to assess cell viability and growth. The viability of human osteogenic sarcoma Saos-2 cells on RP4 electrospun fibers is significantly higher than that on RP1, RP2, and P-*S,S*-LA fibers ($p < 0.05$).

Introduction

Aliphatic polyesters, such as polylactide, polyglycolide, poly(ε-caprolactone), and their copolymers, have been widely used for biomedical applications, including degradable sutures, bone pins, coronary artery stents, controlled drug delivery vectors, and as scaffold materials for regenerative medicine.[1−4] These medical applications rely on the degradability of the polyesters; indeed, they are hydrolyzed in vivo to carboxylic acids which are subsequently metabolized via the citrate cycle. Poly(*S,S*-lactide) (P-*S,S*-LA) is of particular interest and importance because it is commercially produced from renewable resources (*S*-lactic acid is produced by fermentation of D-glucose).[5,6] Thanks to its relatively high mechanical strength, polylactide has been used in orthopedic surgery as a fixation device.[7] In tissue engineering, polylactide is rarely used on its own as the scaffold material due to its poor cell attachment.[8] This can be overcome, to some extent, by fabricating submicrometer-sized fibrous scaffolds, which promote cell adhesion because of the high surface area.[9] However, the biomedical applications of polylactide are frequently restricted by its high crystallinity, hydrophobicity, limited degradation control, and poor cell attachment profile.[1−3]

For tissue engineering applications the high hydrophobicity of polylactide, and related aliphatic polyesters, makes them poorly compatible with biological environments and in some cases leads to undesirable inflammation and foreign body responses.[10,11] Various strategies have been used to increase the hydrophilicity of the polyester, including modifying the chain end-groups,[12−18] copolymerization with hydrophilic monomers,[18−35] control of the macromolecular architecture,[36−44] and surface modification reactions.[45,46] Copolymers of lactide and ethylene glycol have received a great deal of attention as materials for drug delivery and as hydrogels for regenerative medicine.[11,31,47−51] While impressive results have been achieved, the lack of degradability of ethylene glycol and its structural heterogeneity can cause problems. Furthermore, it is desirable to prepare polyesters with functional substituents to improve cell/matrix/scaffold interactions.

Degradable, aliphatic polyesters are best prepared by lactone ring-opening polymerization (ROP). This is attractive because it can be a controlled polymerization enabling the synthesis of block copolymers and producing materials of predictable and controllable composition, molecular weight, polydispersity index, and stereochemistry. One method to introduce functional substituents to tailor the materials properties (e.g., hydrophilicity) and medical applications is via the ROP of functionalized lactones.[18,20−28,52−63] We are particularly interested in the preparation of functionalized lactones from renewable resources, such as carbohydrates, due to the sustainability of the raw materials and the ability to take advantage of naturally high degrees of chemical functionality, stereochemistry, hydrophilicity, and degradability to metabolites. Recently, there have been some interesting examples of the ring-opening polymerization of functionalized lactones derived from renewable resources.[25,54−71] Guan and colleagues reported the ring-opening polymerization

*Corresponding author. E-mail: c.k.williams@imperial.ac.uk.

 Published on Web 08/26/2010

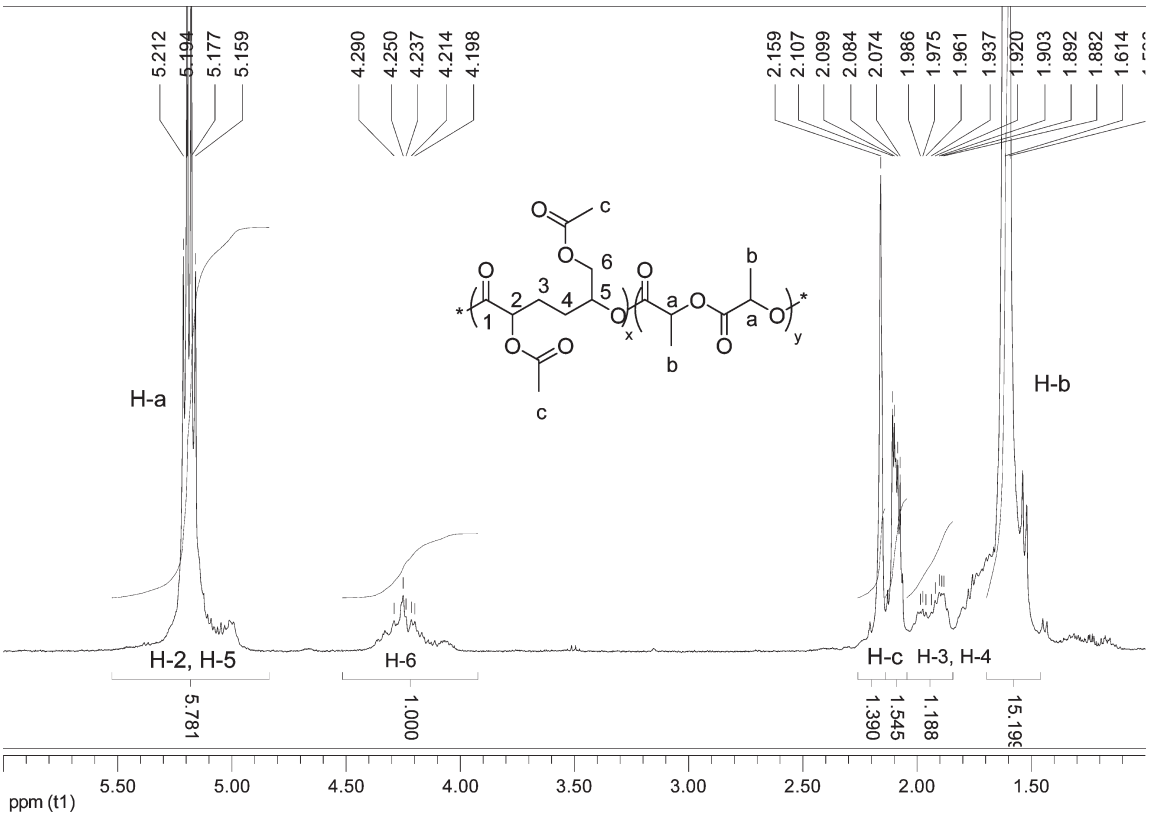

Figure 1. ^{1}H NMR spectrum of RP4 in $CDCl_3$. Polymerization conditions: 25 °C, THF, LZnOEt:**1**:*S,S*-LA, 1:100:200.

Scheme 1. Copolymerization of Monomer 1 and *S,S*-Lactide[a]

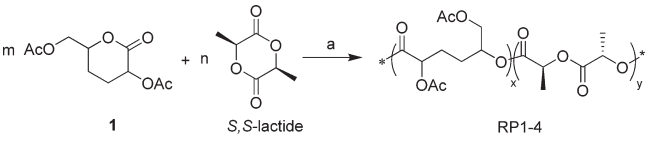

[a] Copolymerization conditions: (a) 25 °C, THF, LZnOEt (structure illustrated in Figure S1), isolated yields = 56%−88%. RP1, m = 10, n = 290; RP2, m = 25, n = 275; RP3, m = 50, n = 250; RP4, m = 100, n = 200. The random copolymers have x:y = 1:99 (RP1), 4:96 (RP2), 7:93 (RP3), and 17:83 (RP4).

of a permethoxylated ε-caprolactone derived from D-dulcitol and its copolymerization with ε-caprolactone.[62] The new materials showed excellent protein resistance.

Previously, we reported a novel carbohydrate lactone **1**, which was prepared in two high yielding steps from commercially available D-gluconolactone.[63] The homopolymer from **1** is hydrophilic, with a static water contact angle of ∼30°. Here we report, the synthesis of a series of random copolymers prepared from **1** and *S,S*-lactide (both derived from abundant, naturally occurring carbohydrates) and the properties of the copolymers, including preliminary results in cell viability studies.

Results and Discussion

Synthesis and Characterization. The random copolymers of monomer **1** and *S,S*-lactide were prepared by ring-opening polymerizations (Scheme 1). The ring-opening polymerization was initiated using a zinc alkoxide complex (for an illustration of chemical structure of the initiator, see Figure S1) which had previously shown excellent activity and control in lactide polymerization.[72] The polymerizations were conducted in THF due to the good solubility of all reagents and products in this solvent. A series of polymerizations were run at increasing ratios of zinc initiator:monomer **1**:*S,S*-lactide, from 1:10:290 to 1:100:200 (see Table S1). The total concentration of the polymerization solutions was always kept at 1 M, which is the most commonly used concentration for lactide ring-opening polymerization experiments.[5] A control experiment was conducted at a loading of zinc initiator:*S,S*-lactide of 1:300 to produce poly(*S,S*-lactide). The polymerizations were quenched, after 15 min of reaction by the addition of diethyl ether (unpurified), which resulted in chain termination (by reaction between the zinc alkoxide and water in the solvent) and in the precipitation of the copolymers.

The crude products were analyzed (after solvent removal) by ^{1}H NMR spectroscopy which showed the copolymers were composed of ring-opened **1** and *S,S*-LA repeat units. The crude ^{1}H NMR spectra all showed a significant quantity of **1** remained unreacted, despite all the *S,S*-lactide having been consumed. It has already been established that the zinc initiator polymerizes *S,S*-lactide in minutes under these conditions (i.e., at 1:100, LZnOEt:*S,S*-LA, [*S,S*-LA] = 1 M in THF),[72] whereas it takes more than 1 h to polymerize **1** under equivalent conditions.[63] It is, therefore, likely that there is some degree of compositional drift in the copolymers.

The copolymers were purified, and the residual monomer **1** was removed by repeated dissolution and precipitation from $CHCl_3$ and diethyl ether. A representative ^{1}H NMR spectrum of one of the purified copolymers is shown in Figure 1; the peaks are assigned, and a numbering scheme for ring-opened **1** is included. There was no evidence for the epimerization of the *S,S*-LA units (as evidenced by the quartet at 5.18 ppm). Monomer **1** is a racemic mixture of the two syn-enantiomers, and these were incorporated in an atactic manner. The relative loadings of ring-opened **1** and *S,S*-lactide in the copolymers were determined by analyzing the peak integrals for a peak solely associated with

Table 1. Characterization and Degradation Data for the Random Copolymers[a]

copolymer	loading[b] LZnOEt:1:*S,S*-LA	MRO **1**%/% (m/m)[c]	WRO **1**%/% (w/w)[d]	M_n(SEC)[e]/g mol^{-1}	PDI	k_x[f]/10^{-4}/D^{-1}	R^2
RP1	1:10:290	1	1	88 000	1.36	1.3	0.99
RP2	1:25:275	4	6	68 000	1.71	2.1	0.99
RP3	1:50:250	7	11	61 000	1.59	2.9	0.99
RP4	1:100:200	17	25	44 000	1.51	4.2	0.99
P-*S,S*-LA	1:0:300	0	0	108 000	1.40	0.9	0.99
P-*S,S*-LA2	1:0:150	0	0	41 000	1.52	0.9	0.99

[a] Copolymerization of **1** and *S,S*-lactide, initiated by LZnOEt (Figure S1) in THF at 25 °C, [*S,S*-lactide] + [**1**] = 1 M. [b] The loadings of reagents and initiator. [c] MRO **1**%: the molar ratio of ring-opened **1** in the copolymer; determined from the ^{1}NMR spectrum by dividing the integration the peaks from 4.0 to 4.5 ppm (ring-opened **1**, H-6 and H-6′) by the integration of the peaks from 4.9 to 5.5 ppm (two methyne protons on lactide, H-2 and H-5 of ring-opened **1**). [d] WRO **1**%: the weight ratio of the ring-opened **1** in the copolymer, calculated from the molar ratio. [e] M_n determined by SEC ($CHCl_3$) using polystyrene standards. [f] The degradation experiment conditions are described in the Experimental Section; the degradation rate constants, k_x, were determined from the gradients of the lines in Figure 3.

ring-opened **1** (δ: 4.00−4.50 ppm, due to the two H-6 protons) and for a peak which is a composite of resonances due to ring-opened **1** and *S,S*-lactide (δ: 4.90−5.50 ppm, due to the two CH protons on the *S,S*-lactide and due to H-2 and H-5 on ring-opened **1**). Table 1 shows the copolymer compositions, as determined by integration of the ^{1}H NMR spectra; copolymers composing between 1 and 25 wt % of ring-opened **1** can be prepared. It shows a lower loading (∼50%) of repeat units of ring-opened **1** than expected on the basis of the reaction stoichiometry (the conversion of monomer **1** is listed in Table S1; some oligomers were formed and removed during the precipitation process), consistent with the relative rates of polymerization of the monomers and the crude ^{1}H NMR spectra. We are confident that copolymers were obtained (and not mixtures of two homopolymers) as it was not possible to change the composition of the copolymers by further solvent extraction/precipitation methods, and the size exclusion chromatography (SEC) data show only a single peak for each of the copolymer samples. Size exclusion chromatography (SEC), in chloroform solution and using narrow M_n polystyrene standards, was used to analyze the copolymer molecular weights. The copolymers had number-average molecular weights between 44 000 and 88 000 g/mol, albeit with relatively broad polydispersity indices. There was a trend toward higher M_n as the proportion of *S,S*-lactide incorporation increased. There are several possible causes for the increase in M_n. First, when the loading of *S,S*-lactide in the feedstock is higher than there are a greater number of repeat units (equivalents of monomer reacted) overall in the copolymer. This is because *S,S*-lactide is completely converted, whereas **1** is only partially converted in the polymerization time. Second, polystyrene standards were used to calibrate the SEC instrument, and the copolymers are expected to show different correction factors vs the polystyrene standards as the compositions change. This latter effect is likely to be dominant but cannot yet be precisely determined because the Mark−Houwink−Sakurada parameters for **1** are unknown. It is therefore expected that the hydrodynamic volumes of the copolymers change with their composition. In fact, it has already been reported that poly(*S,S*-lactide) requires a correction factor of ∼0.58 when polystyrene calibrants are used in THF solutions.[73] Finally, we cannot rule out some transesterification reactions between the acetyl substituents and the polymer chains, leading to chains with variable substituent chain length and/or some degree of chain branching leading to differing polymer macrostructures. These uncertainties mean that the M_n values should be treated only as approximate estimates.

Thermal Properties. Differential scanning calorimetry (DSC) and thermal gravimetric analysis (TGA) have been used to characterize the random copolymers. This is particularly important as any processing scenario must take into consideration the thermal stability of the materials. TGA shows the degradation of the homopolymer from **1** begins at 250 °C.[63] P-*S,S*-LA is thermally stable up to ∼290 °C.[74] The weight loss onset temperatures of the copolymers are between 250 and 290 °C; the degradation temperature decreases as the loading of **1** in the copolymer increases (the plots are illustrated in Figure S2).

Table 2. Comparison of the Glass Transition Temperatures for the Copolymers Determined Experimentally[a] and Theoretically, and the Onset Degradation Temperatures

copolymer	WRO **1**%/% (w/w)[b]	calc T_g/°C[c]	T_g(DSC)/ °C	T_m(DSC)/ °C	T_d(TGA)/ °C[d]
RP1	1	57.0	55.1	167.2	290.4
RP2	6	54.7	53.7	160.5 (151.4)	281.6
RP3	11	52.2	52.2	155.7 (145.0)	279.1
RP4	25	46.8	46.0	N	255.0

[a] DSC experiments were used to determine the thermal properties for each copolymer sample. Each measurement was carried out over three heating and cooling cycles, with the samples being heated to 200 at 10 °C/min and cooled to −40 at 10 °C/min. In all cases, the second and third cycles gave reproducible analyses. The data used were from the second heating cycle; a representative analysis is illustrated in Figure S3. [b] WRO **1**%: the weight ratio of the ring-opened **1** in the copolymer, calculated from the molar ratio. [c] The T_g is calculated from the Fox equation. [d] Degradation temperature. Thermogravimetric analysis was carried out on Pyris 1 TGA (PerkinElmer, UK), under air flow (20.0 mL/min) at a heating rate of 10 °C/min from 50 to 500 °C. The reported data are the onset degradation temperatures of the samples.

Also, the crystallinity of the material will have important implications for the degradation rates and subsequent applications of the materials. In order to study the random copolymers' thermal properties, the glass transition temperature of homopolymer **P1** had to be established (see Supporting Information): it was 29.6 °C. The glass transition temperatures of the copolymers are expected to obey the Fox equation (1), where $T_{g,a}$ is the glass transition temperature of **P1** (29.6 °C/302.8 K); $T_{g,b}$ is the glass transition temperature of P-*S,S*-LA (57.8 °C/331.1 K), determined by measuring the P-*S,S*-LA homopolymer (monomer:initiator, 300:1) under the same conditions as for the copolymers, the value agrees well with literature values for P-*S,S*-LA T_g;[75] w_a is the weight fraction of ring-opened **1**; and w_b is the weight fraction of ring-opened *S,S*-LA.

$$\frac{1}{T_g} = \frac{w_a}{T_{g,a}} + \frac{w_b}{T_{g,b}} \quad (1)$$

Table 2 compares the glass transition temperatures predicted from the Fox equation for the various copolymer compositions. The DSC results show that the glass transition temperatures of the copolymers increase as the *S,S*-lactide

proportion increases (Table 2). There is an excellent agreement between the experimentally determined glass transition temperatures and those predicted from the Fox equation. For RP4, no melting temperatures were observed; for sample RP1, one melting peak was observed, the melting temperature was slightly lower than P-*S,S*-LA; but for samples RP2 and RP3, there are two melting peaks, consistent with these species being semicrystalline copolymers.[76] It suggests there is some microphase separation of the *S,S*-LA and **1** portions in these copolymers. Compared with the melting temperature of P-*S,S*-LA (174.4 °C), the melting temperatures of the crystalline domains in the copolymers are lower consistent with a reduction in the degree of crystallinity by ring-opened monomer **1** (e.g., Figure S3). This suggests that when the *S,S*-lactide incorporation is sufficiently high (>80%, w/w), microphase separation occurs in the copolymers. On the other hand, when the proportion of ring-opened **1** exceeds 20%, w/w, there is no microphase separation, and thus no melting temperature is observed.

Static Water Contact Angle Measurements. Films of the copolymers were prepared by spin-coating chloroform solutions of the copolymers (30 mg/mL in $CHCl_3$, 200 μL) onto glass slides (Φ = 32 mm), at a rate of 1500 rpm for 2.5 min. The films were dried, under vacuum at 25 °C for 20 h before the static water contact angles were determined. The static water contact angles of the films depended on the proportion of ring-opened **1** in the copolymer, with the angle decreasing with increasing content of **1** (Figure 2a). The static contact angles vary from ~79.1° for P-*S,S*-LA to 71.4° for RP4. This trend is to be expected as monomer **1** contains functional substituents which are expected to increase the hydrophilicity of the materials. The copolymers were also electrospun, from hexafluoroisopropanol (HFIP) solutions, to yield fibers of < 1 μm diameter. The static water contact angles of all the copolymer fiber samples exceed 120°, and again, increasing the proportion of ring-opened **1** in the copolymer increases the surface hydrophilicity. The higher water contact angles observed for the fibers are caused by the high surface roughness of the fibrous meshes.[77] This phenomenon is commonly known as the Cassie−Baxter state.[78] For materials with a water contact angle lower than 90° on a smooth surface, the Cassie−Wenzel transition is expected to occur when water penetrates the porous matrix, leading to a significant reduction in the water contact angle.[79] In this study, the transition was not observed before the complete evaporation of the water droplet, indicating the Cassie−Baxter state is metastable.[80]

Degradation of the Copolymers. It is well-known that many aliphatic polyesters, including P-*S,S*-LA, are relatively slow to degrade, and this can be problematic for certain applications.[1−3] Furthermore, solid samples of P-*S,S*-LA (e.g., for packaging applications) need to be above the glass transition temperature (56 °C) in order for the degradation to proceed at all. This creates some significant problems for PLA application and marketing as degradation will only actually occur in industrial composting conditions and not using domestic composting. For biological applications there are also applications such as drug delivery or tissue scaffolding for which faster PLA degradation could be beneficial.[3,4] P-*S,S*-LA was reported to have a half-life of 110 weeks,[81] which is not optimum for many drug delivery and tissue engineering uses. The degradation reaction is an ester hydrolysis and so depends on the rate of water uptake into the material; it is strongly affected by the polymer's hydrophilicity and crystallinity.

The incorporation of **1** into copolymers with *S,S*-lactide is expected to increase the degradation rate compared to poly(*S,S*-lactide) as it will increase the hydrophilicity of the material. Furthermore, we have already shown that the copolymers have decreased T_g and T_m vs P-*S,S*-LA, which is expected to further facilitate water uptake and increase the degradation rate. As a preliminary investigation of the degradation characteristics of the random copolymers, the degradation was carried out in solution (in $CHCl_3$, with phosphate buffered saline solution) and monitored using SEC. The buffer was added to prevent any buildup of acidic byproduct and to prevent an autocatalytic degradation mechanism. The degradation assay is biphasic, and the partition coefficient between the aqueous and chlorinated phases is expected to contribute to the absolute degradation rate. Nevertheless, it was a useful degradation assay as it enabled quantification of the degradation rates and comparisons between the random copolymer structures in a manageable time scale. It should be noted that the absolute rate constants obtained from this experiment may not directly correlate with how long it takes a sample to degrade in soil/in vivo as the degradation rate will depend on the material's size, processing history, use, and the degradation medium, among other factors. However, the method is useful because it accurately illustrates the trends in rate constant and in particular the effect of incorporating greater quantities of **1** on the degradation rate of the material.

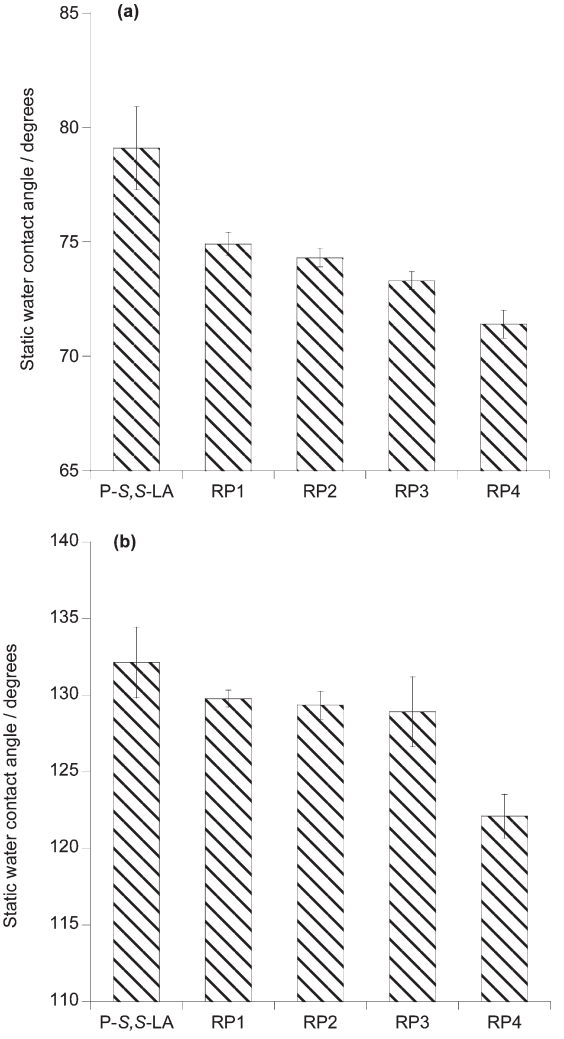

Figure 2. (a) Static water contact angles of the copolymer films (the data are expressed as mean ± SD, n = 16). (b) Static water contact angles of the copolymer fibers (the data are expressed as mean ± SD, n = 8).

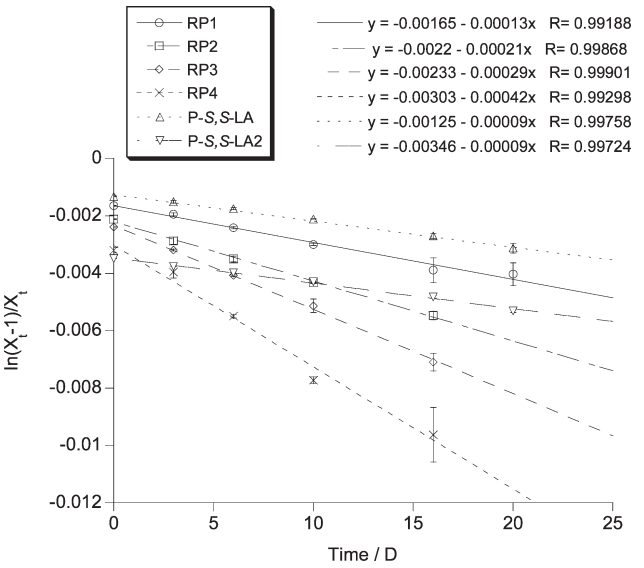

Figure 3. Plots of $\ln((X_t - 1)/X_t)$ vs time for the copolymers (Table 1). The degradation experimental conditions are described in the Experimental Section. Each degradation experiment was conducted three times, and the errors for each measurement are included.

The degradation occurs by a random chain scission mechanism under these conditions, a mechanism which is common to other aliphatic polyester degradations.[82] Liu et al. showed that for P-*S,S*-LA the number-average degree of polymerization at time t (X_t) can be related to the initial degree of polymerization (X_0), the time, and the degradation rate constant (k_x) according to eq 2.[82]

$$\ln\frac{X_t - 1}{X_t} = \ln\frac{X_0 - 1}{X_0} - k_x t \qquad (2)$$

Using eq 2, plots of $\ln\{(X_t - 1)/X_t\}$ vs time were constructed for the various copolymer samples (Figure 3); the gradients of the linear fits to the data correspond to $-k_x$. Each copolymer degradation experiment was repeated three times, and the errors in each data point are included in Figure 3. It is observed that as the quantity of ring-opened **1** in the copolymer increases (going from copolymer RP1 to RP4), so the degradation rate increases and that the homopolymer of *S,S*-lactide (P-*S,S*-LA) has the slowest degradation rate (Figure 4). However, the random copolymer samples' molecular weights also differ, as discussed previously. In order to quantify the influence, if any, of the polymer molecular weight on the degradation reaction, two samples of P-*S,S*-LA were prepared with number-average molecular weights at either end of the range observed for the copolymers, i.e., with M_n = 41 000 and 108 000 g/mol, respectively. Both samples have the same degradation rate constants, implying that over this range, and under these degradation conditions, the influence of molecular weight on the degradation rate is minimal. Therefore, the enhanced degradation rates of the copolymers containing ring-opened **1** are tentatively attributed to its greater hydrophilicity compared to P(*S,S*-LA) which is, in turn, expected to increase the rate of ester hydrolysis. There is a linear correlation between the quantity of ring-opened **1** in the copolymer samples and the degradation rate constants (Figure 4). The ability to accurately control and predict the degradation rates of a material by changing its chemical composition is potentially significant for biomedical applications. For example, the controlled release of an active compound from a polymeric vector could be controlled by changing the degradation rate of the polymer backbone.

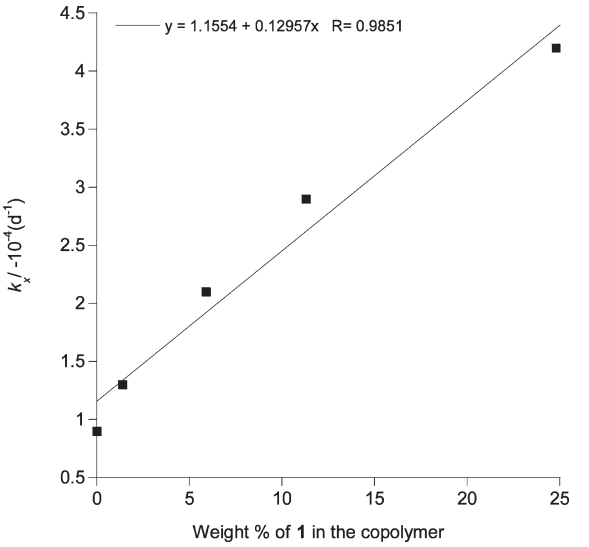

Figure 4. Plot of the degradation rate constant, k_x, vs the weight percentage of ring-opened **1** in the copolymer samples.

For tissue engineering, an ideal scaffold material should have a degradation rate matching the corresponding tissue regeneration, and therefore materials with tunable degradation rates are of considerable interest.

Cell Attachment and Viability. Electrospinning is a widely used technique to fabricate tissue engineering fibrous scaffolds.[83] The fiber size produced by electrospinning ranges from 100 nm to a few micrometers, resembling the structure of native extracellular matrix (ECM).[84] In this study, the copolymers were electrospun into a fibrous scaffold to investigate their potential in tissue engineering. Saos-2 cells, from a human osteosarcoma cell line commonly used in bone tissue engineering studies,[85] were cultured on the scaffolds to investigate the cytotoxicity/biocompatibility. Representative LIVE/DEAD staining images of Saos-2 cells cultured on the two different electrospun scaffolds for 5 days are shown in Figure 5 (all samples illustrated in Figure S5). More than 90% of the Saos-2 cells were viable on each type of scaffold. However, SEM images (Figure 5) indicated that the Saos-2 cells tend to spread more on RP4 fibers as compared to cells on the P-*S,S*-LA fibers, which exhibited rounded cell shapes. RP4, with a higher ratio of ring-opened **1**, is more hydrophilic due to the increased incorporation of hydrophilic functional groups. We postulate that this could facilitate cell attachment and spreading.

The MTS assay supported the LIVE/DEAD data (Figure 6). The cell viabilities were higher on RP3 and RP4 fibers compared to those on RP1, RP2, and P-*S,S*-LA fibers. From day 5 onward, the metabolic activities of Saos-2 cells on the RP4 electrospun fibers were significantly higher than those on the RP1, RP2, and P-*S,S*-LA fibers ($p < 0.05$). There is also a trend toward increased cell viabilities with increased proportion of ring-opened **1** in the copolymer. Again, it is proposed that scaffolds with a higher content of ring-opened **1** are more hydrophilic and therefore result in higher cell viability. Although the static water contact angles determined for the fibrous scaffolds are high (Figure 2b), the scaffolds supported cell adhesion and proliferation well. It is possible that the cells are too small to sense the apparent hydrophobicity of the scaffolds on the macroscale. Therefore, the cell adhesion might not be affected by the apparent high hydrophobicity of the fibrous scaffolds, but it could be more sensitive to the intrinsic hydrophilicity or chemistry of the copolymers.

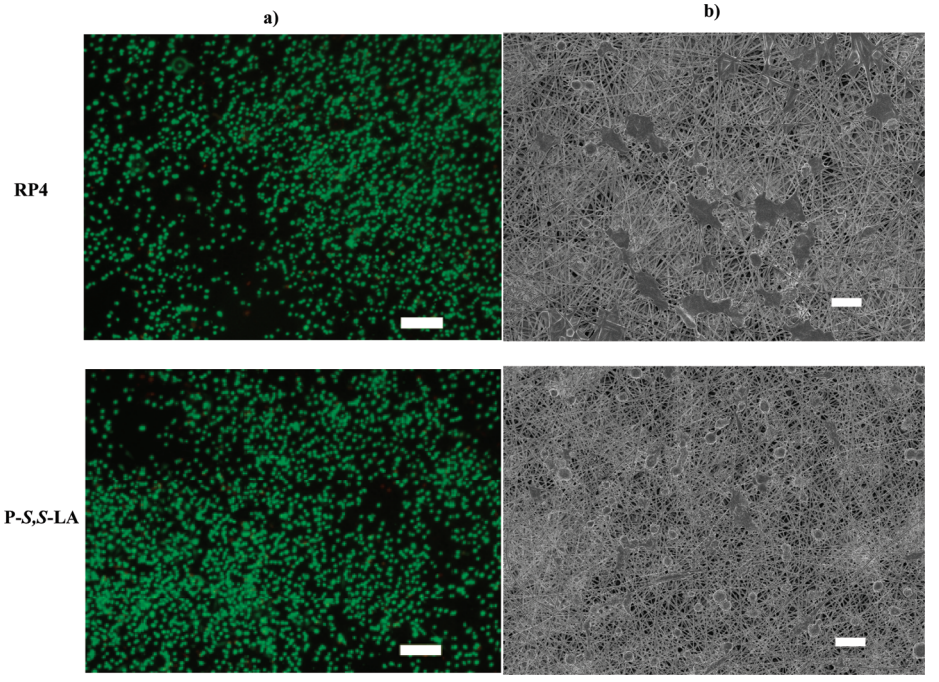

Figure 5. (a) LIVE/DEAD staining of Saos-2 cells on RP4 and P-*S,S*-LA electrospun fibers after 5 days of culture (scale bar: 200 μm). (b) SEM images of Saos-2 cells on RP4 and P-*S,S*-LA electrospun fibers after 5 days of culture (scale bar: 20 μm).

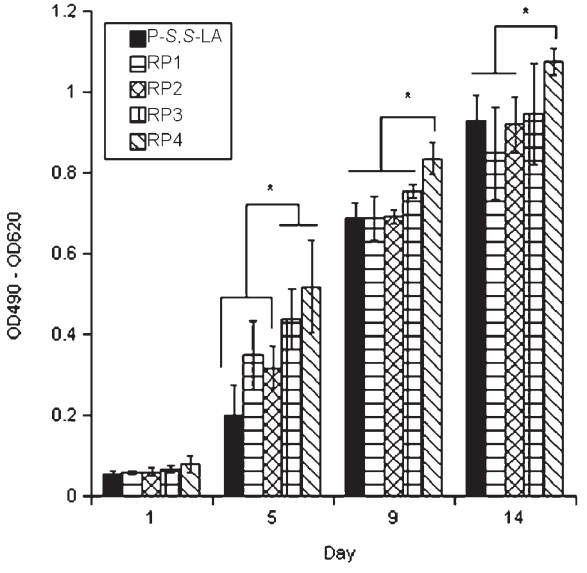

Figure 6. MTS assays on Saos-2 cells cultured for 1, 5, 9, and 14 days. The *y*-axis is the difference between optical density at 490 nm and optical density at 620 nm. * indicates significant difference ($p < 0.05$).

As mentioned, the slow degradation and high hydrophobicity of degradable polyesters, such as P-*S,S*-LA, limits applications in medicine. Copolymerization is a common approach to modulate the polyester properties, with copoly(ester−ethylene glycol) materials being very widely studied.[11,31,47−51] The ethylene glycol portions have been used to significantly increase the aqueous wettability of electrospun copolymer scaffolds, resulting in enhanced cellular attachment and proliferation. In this study, an alternative degradable and renewable monomer (**1**) was copolymerized with *S,S*-LA to produce copolymers with related properties. An advantage of using the carbohydrate-derived lactone, **1**, is that it has two functional substituents per repeat unit. An important challenge for the future development of scaffold materials for regenerative medicine lies in developing methods to incorporate bioactive species, e.g., enzymes/proteins, into the degradable matrix. The new copolymers presented here may offer the potential for the attachment of such groups to the copolymer backbone.

Conclusions

The preparations of a series of random copolymers of a carbohydrate lactone (compound **1**) and *S,S*-lactide have been reported. The lactones both derive from annually renewable resources, which are inexpensive, abundant, and of low toxicity. The random copolymers incorporated up to 25 wt % of ring-opened **1** with ring-opened *S,S*-LA. The loading of **1** was estimated by integration of the ^{1}H NMR spectrum. The copolymers were also analyzed by SEC which showed increasing M_n with increasing LA incorporation into the structures. The copolymers showed glass transition temperatures in the range 40−60 °C, depending on the loading of ring-opened **1**, and showed an excellent correlation with the values predicted from the Fox equation. At low loadings of ring-opened **1** in the copolymers, microphase separation occurred, leading to formation of semicrystalline domains of P-*S,S*-LA and melting temperatures being observed by DSC. When the loading of ring-opened **1** exceeded 20%, an amorphous copolymer was formed. The incorporation of the carbohydrate lactone increased the hydrophilicity of the copolymer, as indicated by the decrease in the water contact angle. The incorporation of ring-opened **1** also modified the degradation rate of the copolymers; as the loading of ring-opened **1** increased, so the degradation rate increased. This phenomenon was attributed to the increased hydrophilicity of copolymers containing higher proportions of ring-opened **1**. The cell culture experiments, on electrospun fibers of the copolymers, showed that RP4 permitted good cell attachment and cell metabolic activity, highlighting the potential for these new materials in regenerative medicine.

Experimental Section

Materials. Compound **1** and the initiator LZnOEt (see Figure S1 for the structure) were prepared and purified according to the

literature methods.[63,72] *S,S*-Lactide was donated by Purac Plc, it was purified by recrystallization from hot toluene followed by repeated sublimation in vacuo (three times). All the compounds were stored in an M-Braun glovebox. THF was distilled from sodium and stored under nitrogen. Chloroform-d_3 was dried by distilling it from calcium hydride, performing three freeze−thaw cycles under vacuum, and it was stored under nitrogen. Hexafluoroisopropanol (HFIP) was purchased from Sigma and used as received.

Characterization. NMR spectra were carried out on a Bruker AV500 instrument; ^{1}H NMR spectra were collected at 500 MHz. $CDCl_3$ was used as the NMR solvent and reference compound. The SEC measurements were performed on a Polymer Laboratories SEC 50 instrument with two Polymer Laboratories mixed D columns and $CHCl_3$, at a flow rate of 1 mL min^{-1}, as the eluent. Narrow molecular weight polystyrene standards (Polymer laboratories, mixed A and B) were used to calibrate the instrument. The thermal properties were measured using differential scanning calorimetry (Diamond DSC, Perkin-Elmer, UK). Scans were performed from −70 to 170 °C at a controlled heating rate of 10 °C/min. A sealed empty crucible was used as a reference, and the DSC was calibrated using indium. The thermal gravimetric analysis (Pyris 1 TGA, Perkin-Elmer, UK) was carried out in flowing air at a heating rate of 10 °C/min. Static water contact angles were measured using a drop shape analysis system (EasyDrop, Krüss, Germany). A 2 μL drop of ultrapure water (Milli-Q water, Millipore, MA) was placed on the polymer surfaces, and the static water contact angle was measured. The measurements were performed on several different areas of each sample, repeated on two samples for each kind of polymer film, and the values averaged. The cell morphology and adhesion were investigated using SEM (LEO 1525, Zeiss, UK). The colorimetric change was measured by a spectrophotometric plate reader (Anthos 2020 Microplate Readers, Biochrom Ltd., UK) and a Glassman high-voltage generator (PS/EL30R1.5, Glassman).

Copolymer Syntheses (Representative Example: The Synthesis of RP4). Stock solutions of *S,S*-lactide (1 M) and the initiator LZnOEt (0.025 M) were made separately in THF. Compound **1** (0.575 g, 2.500 mmol) was added to an oven-dried vial with a stirrer. Then the stock solution of *S,S*-lactide (5 mL) was added, followed by the addition of sufficient THF (1.5 mL) to ensure that the overall concentration was 1 M (i.e., [**1**] + [*S,S*-LA] = 1 M). The mixture was stirred until everything dissolved. Then, the stock solution of LZnOEt (1 mL) was added into the monomer solution. The reaction was stopped after 15 min, the vial was exposed to air, and the addition of wet diethyl ether (i.e., straight from the Winchester) caused precipitation of the copolymer. The polymer was purified by repeated dissolution and precipitation ($CHCl_3$ and diethyl ether, 3×) and dried under vacuum to yield a white solid (0.72 g, 56%). ^{1}H NMR (400 MHz) δ: 4.9−5.6 (m, OCH(CH_3)CO, H-2, H-5); 4.0−4.4 (m, H-6, H-6′); 2.12−2.22 (s, $COCH_3$); 2.04−2.12 (m, $COCH_3$); 1.60−2.05 (m, H-3, H-3′, H-4, H-4′); 1.45−1.60 (d, $CHCH_3$) ppm. SEC($CHCl_3$, 1 mL/min), M_n = 44 000 g/mol, PDI = 1.51.

The same general procedure was used for the preparation of RP1−3. The quantities of monomers, initiators, and isolated polymer yields are listed in Table S1.

Thermal Analyses. The thermal properties were measured using differential scanning calorimetry (Diamond DSC, Perkin-Elmer, UK). Scans were performed from −70 to 170 °C, at a controlled heating and cooling rate of 10 °C/min. A sealed empty crucible was used as a reference, and the DSC was calibrated using indium. Each sample was run for three heating−cooling cycles. After the first cycle, the DSC traces of the second and third cycles were identical. The glass transtion temperatures reported are taken from the second cycle. Thermogravimetric analyses were carried out using a Pyris 1 TGA instrument (PerkinElmer, UK), under air flow (20.0 mL/min), at a heating rate of 10 °C/min from 50 to 500 °C.

Degradation Experiments. The copolymer (2 mg) was dissolved in $CHCl_3$ (1 mL), and phosphate buffered saline solution (PBS, 24 mM Na_2HPO_4 and 16 mM KH_2PO_4 in 0.9% NaCl, pH = 7.4, 0.1 mL) was added to the samples. The samples were kept in a 25 °C water bath and were shaken every few hours. SEC was used to determine the M_n of the degrading copolymer samples.

Spin-Coating. RP1, RP2, RP3, RP4, and P-*S,S*-LA powder (30 mg) were dissolved in $CHCl_3$ (1 mL). A round glass slide (Φ = 32 mm) was placed on the center of the spin-coater (Laurell, WS-650SZ-6NPP/LITE), and the polymer solution (200 μL) was spread on it. The machine span to the plate was spun at a rate of 1500 rpm for 2.5 min. The coated films were dried under vacuum at 25 °C for 20 h before the determination of the contact angles.

Electrospinning. RP1, RP2, RP3, RP4, and P-*S,S*-LA solutions were prepared by dissolving the polymers in HFIP at a concentration of 18%, 17%, 17%, 25%, and 15% (w/v), respectively. The solutions were placed in a plastic syringe fitted with a 27G1/2 needle (Becton Dickinson). A high dc voltage (7 kV) was applied between the needle and the collecting plate (distance = 12 cm) with a high-voltage power supply (Glassman High Voltage). The solution was delivered at a constant feed rate of 0.5 mL/h. 15 cm round cover glasses (VWR) were placed on top of the aluminum collecting plate. The resultant electrospun fibers were collected on the cover glass. The cover glasses with fibers were used for cell culture in 24-well plates. The fiber diameters were 947 ± 95, 796 ± 113, 762 ± 147, 808 ± 233, and 770 ± 95 nm, respectively, as measured by SEM (n = 100).

Cell Culture. Cells of the human osteosarcoma cell line (Saos-2) were cultured in an RPMI medium containing 10% (v/v) fetal bovine serum (FBS) and L-glutamine (2 mM). The medium was replaced every 2 days, and the cultures were maintained in a humidified incubator at 37 °C with 5% CO_2. When the cells reached 80−90% confluence (5×10^4 cells/cm^2), the cultures were trypsinized and subcultured at 1:3 ratios. For cell culture experiments, the electrospun fiber samples were placed in 24-well plates and sterilized with a 70% ethanol solution for 30 min, followed by three washes with 1X PBS. The cells were seeded onto the electrospun fibers at a seeding density of 1.2×10^4 cells/cm^2 and cultured for desired periods to evaluate cell metabolism.

LIVE/DEAD Staining and MTS Assay. Electrospun fiber samples seeded with Saos-2 cells were kept at 37 °C in the 5% CO_2 atmosphere for incubation periods of 1, 5, 9, and 14 days. At each time point, the samples were collected for LIVE/DEAD staining and MTS assay.

For LIVE/DEAD staining, the samples were washed with PBS. Then 300 μL of LIVE/DEAD assay solution (Invitrogen), which contained 1 μM ethidium homodimer-1 (Ethd-1) and 1 μM Calcein AM in PBS, was added to each well. After 30 min in 25 °C, the samples were viewed under a fluorescence microscope. The live cells were stained with calcein, which is excited at the wavelength of 485 nm and emits at 530 nm. The dead cells were stained by EthD-1, which is excited at 530 nm and emits at 645 nm.

For the cell metabolic activity assessment, at different intervals, unattached cells were removed by washing and the metabolic activity was quantified by the colorimetric MTS assay (CellTiter 96 AQueous One Solution Cell Proliferation Assay, Promega). Briefly, the cell−fiber samples were incubated with 20% (v/v) MTS reagent in complete medium for 3 h. Thereafter, aliquots (in triplicates) were transferred to a 96-well plate, and the reduction of the tetrazolium salt as indicated by colorimetric change was determined by measuring the absorbance at 490 nm with a spectrophotometric plate reader, with subtraction of the background absorbance at 620 nm.

Scanning Electron Microscopy (SEM). SEM was used to examine the morphologies of fibers and cells cultured on the electrospun scaffolds. The cell−fiber samples were washed with PBS to remove nonadherent cells. The adherent cells were fixed

with 2.5% (v/v) glutaraldehyde for 45 min at 4 °C. Thereafter, the samples were sequentially dehydrated in 50, 70, 80, 90, 95, and 100% ethanol solutions for 5 min each and vacuum-dried. The samples were sputter-coated with chromium (K575X, Emitech, UK) and observed under a field-emission scanning electron microscope (Leo 1525) at an accelerating voltage of 5 kV.

Acknowledgment. The EPSRC is acknowledged for financial support (EP/H00713*X*/1, EP/C544846/1, EP/C544838/1, EP/E007627/1). M.M.S. acknowledges ERC FP7 grant "Naturale" for financial support.

Supporting Information Available: Figures showing the molecular structure of the zinc initiator complex; the DSC analysis of copolymer sample RP3 and thermal gravimetric analyses of the copolymer samples; table showing the quantities of monomers, initiators, and isolated polymer yields. This material is available free of charge via the Internet at http://pubs.acs.org.

References and Notes

(1) Vert, M. *Biomacromolecules* **2005**, *6*, 538–546.
(2) Albertsson, A. C.; Varma, I. K. *Biomacromolecules* **2003**, *4*, 1466–1486.
(3) Place, E. S.; George, J. H.; Williams, C. K.; Stevens, M. M. *Chem. Soc. Rev*. **2009**, *38*, 1139–1151.
(4) Place, E. S.; Evans, N. D.; Stevens, M. M. *Nature Mater*. **2009**, *8*, 457–470.
(5) Platel, R. H.; Hodgson, L. M.; Williams, C. K. *Polym. Rev*. **2008**, *48*, 11–63.
(6) Ragauskas, A. J.; Williams, C. K.; Davison, B. H.; Britovsek, G.; Cairney, J.; Eckert, C. A.; Frederick, W. J., Jr.; Hallett, J. P.; Leak, D. J.; Liotta, C. L.; Mielenz, J. R.; Murphy, R.; Templer, R.; Tschaplinski, T. *Science* **2006**, *311*, 484–489.
(7) Gupta, A. P.; Kumar, V. *Eur. Polym. J*. **2007**, *43*, 4053–4074.
(8) Wang, S.; Cui, W.; Bei, J. *Anal. Bioanal. Chem*. **2005**, *381*, 547–556.
(9) Dong, Y.; Liao, S.; Ngiam, M.; Chan, C. K.; Ramakrishna, S. *Tissue Eng., Part B* **2009**, *15*, 333–351.
(10) Rotter, N.; Ung, F.; Roy, A. K.; Vacanti, M.; Eavey, R. D.; Vacanti, C. A.; Bonassar, L. J. *Tissue Eng*. **2005**, *11*, 192–200.
(11) Kissel, T.; Li, Y.; Unger, F. *Adv. Drug Delivery Rev*. **2002**, *54*, 99–134.
(12) Yasugi, K.; Nakamura, T.; Nagasaki, Y.; Kato, M.; Kataoka, K. *Macromolecules* **1999**, *32*, 8024–8032.
(13) Nagasaki, Y.; Yasugi, K.; Yamamoto, Y.; Harada, A.; Kataoka, K. *Biomacromolecules* **2001**, *2*, 1067–1070.
(14) Ouchi, T.; Uchida, T.; Ohya, Y. *Macromol. Biosci*. **2001**, *1*, 371–375.
(15) Bernard, K.; Degée, P.; Dubois, P. *Polym. Int*. **2003**, *52*, 406–411.
(16) Ouchi, T.; Ohya, Y. *J. Polym. Sci., Part A: Polym. Chem*. **2004**, *42*, 453–462.
(17) Tang, M.; Haider, A. F.; Minelli, C.; Stevens, M. M.; Williams, C. K. *J. Polym. Sci., Part A: Polym. Chem*. **2008**, *46*, 4352–4362.
(18) Williams, C. K. *Chem. Soc. Rev*. **2007**, *36*, 1573–1580.
(19) Barakat, I.; Dubois, P.; Jerome, R.; Teyssie, P.; Goethals, E. *J. Polym. Sci., Part A: Polym. Chem*. **1994**, *32*, 2099–2110.
(20) Tian, D.; Dubois, P.; Jérôme, R. *Macromolecules* **1997**, *30*, 1947.
(21) Trollsas, M.; Lee, V. Y.; Mecerreyes, D.; Lowenhielm, P.; Moller, M.; Miller, R. D.; Hedrick, J. L. *Macromolecules* **2000**, *33*, 4619–4627.
(22) Lou, X.; Detrembleur, C.; Jérôme, R. *Macromol. Rapid Commun*. **2003**, *24*, 161–172.
(23) Rieger, J.; Bernaerts, K. V.; Du Prez, F. E.; Jerome, R.; Jerome, C. *Macromolecules* **2004**, *37*, 9738–9745.
(24) Taniguchi, I.; Mayes, A. M.; Chan, E. W. L.; Griffith, L. G. *Macromolecules* **2005**, *38*, 216–219.
(25) Parzuchowski, P. G.; Grabowska, M.; Tryznowski, M.; Rokicki, G. *Macromolecules* **2006**, *39*, 7181–7186.
(26) Leemhuis, M.; van Nostrum, C. F.; Kruijtzer, J. A. W.; Zhong, Z. Y.; ten Breteler, M. R.; Dijkstra, P. J.; Feijen, J.; Hennink, W. E. *Macromolecules* **2006**, *39*, 3500–3508.
(27) Jiang, X. W.; Smith, M. R.; Baker, G. L. *Macromolecules* **2008**, *41*, 318–324.
(28) Seyednejad, H.; Vermonden, T.; Fedorovich, N. E.; van Eijk, R.; van Steenbergen, M. J.; Dhert, W. J. A.; van Nostrum, C. F.; Hennink, W. E. *Biomacromolecules* **2009**, *10*, 3048–3054.
(29) Jeong, B.; Bae, Y. H.; Lee, D. S.; Kim, S. W. *Nature* **1997**, *388*, 860–862.
(30) Han, D. K.; Hubbell, J. A. *Macromolecules* **1997**, *30*, 6077–6083.
(31) Otsuka, H.; Nagasaki, Y.; Kataoka, K. *Biomacromolecules* **2000**, *1*, 39–48.
(32) Arimura, H.; Ohya, Y.; Ouchi, T. *Biomacromolecules* **2005**, *6*, 720–725.
(33) Mahmud, A.; Xiong, X. B.; Aliabadi, H. M.; Lavasanifar, A. *J. Drug Targeting* **2007**, *15*, 553–584.
(34) Deng, C.; Chen, X. S.; Sun, J.; Lu, T. C.; Wang, W. S.; Jing, X. B. *J. Polym. Sci., Part A: Polym. Chem*. **2007**, *45*, 3218–3230.
(35) Mert, O.; Doganci, E.; Erbil, H. Y.; Dernir, A. S. *Langmuir* **2008**, *24*, 749–757.
(36) Deng, F.; Bisht, K. S.; Gross, R. A.; Kaplan, D. L. *Macromolecules* **1999**, *32*, 5159–5161.
(37) Liu, M.; Vladimirov, N.; Fréchet, J. M. J. *Macromolecules* **1999**, *32*, 6881–6884.
(38) Finne, A.; Albertsson, A.-C. *Biomacromolecules* **2002**, *3*, 684–690.
(39) Cai, Q.; Zhao, Y.; Bei, J.; Xi, F.; Wang, S. *Biomacromolecules* **2003**, *4*, 828–834.
(40) Isabelle, Y.; Degée, P.; Philippe, D.; Jan, L.; Andrzej, D.; Stanislaw, P. *Macromol. Chem. Phys*. **2003**, *204*, 171–179.
(41) Kricheldorf, H. R.; Hachmann-Thiessen, H.; Schwarz, G. *Biomacromolecules* **2004**, *5*, 492–496.
(42) Gottschalk, C.; Frey, H. *Macromolecules* **2006**, *39*, 1719–1723.
(43) Gottschalk, C.; Wolf, F.; Frey, H. *Macromol. Chem. Phys*. **2007**, *208*, 1657–1665.
(44) Dove, A. P. *Chem. Commun*. **2008**, 6446–6470.
(45) Edlund, U.; Källrot, M.; Albertsson, A.-C. *J. Am. Chem. Soc*. **2005**, *127*, 8865.
(46) Quirk, R.; Davies, M.; Tendler, S.; Chan, W.; Shakesheff, K. *Langmuir* **2001**, *17*, 2817–2820.
(47) Li, S. M.; Rashkov, I.; Espartero, J. L.; Manolova, N.; Vert, M. *Macromolecules* **1996**, *29*, 57–62.
(48) Rashkov, I.; Manolova, N.; Li, S. M.; Espartero, J. L.; Vert, M. *Macromolecules* **1996**, *29*, 50–56.
(49) Jeong, B.; Kim, S. W.; Bae, Y. H. *Adv. Drug Delivery Rev*. **2002**, *54*, 37–51.
(50) Kim, K.; Yu, M.; Zong, X. H.; Chiu, J.; Fang, D. F.; Seo, Y. S.; Hsiao, B. S.; Chu, B.; Hadjiargyrou, M. *Biomaterials* **2003**, *24*, 4977–4985.
(51) Tew, G. N.; Sanabria-DeLong, N.; Agrawal, S. K.; Bhatia, S. R. *Soft Matter* **2005**, *1*, 253–258.
(52) Trimaille, T.; Möller, M.; Gurny, R. *J. Polym. Sci., Part A: Polym. Chem*. **2004**, *42*, 4379–4391.
(53) Gerhardt, W. W.; Noga, D. E.; Hardcastle, K. I.; Garcia, A. J.; Collard, D. M.; Weck, M. *Biomacromolecules* **2006**, *7*, 1735–1742.
(54) Vert, M. *Polym. Degrad. Stab*. **1998**, *59*, 169–175.
(55) Marcincinova Benabdillah, K.; Coudane, J.; Boustta, M.; Engel, R.; Vert, M. *Macromolecules* **1999**, *32*, 8774–8780.
(56) Marcincinova-Benabdillah, K.; Boustta, M.; Coudane, J.; Vert, M. *Biomacromolecules* **2001**, *2*, 1279–1284.
(57) Pinilla, I. M.; Martínez, M. B.; Galbis, J. A. *Carbohydr. Res*. **2003**, *338*, 549–555.
(58) Coulembier, O.; Mespouille, L.; Hedrick, J. L.; Waymouth, R. M.; Dubois, P. *Macromolecules* **2006**, *39*, 4001–4008.
(59) Fernández, C. E.; Mancera, M.; Holler, E.; Galbis, J. A.; Muñoz-Guerra, S. *Polymer* **2006**, *47*, 6501–6508.
(60) Liu, T.; Simmons, T. L.; Bohnsack, D. A.; Mackay, M. E.; Smith, M. R.; Baker, G. L. *Macromolecules* **2007**, *40*, 6040–6047.
(61) Haider, A. F.; Williams, C. K. *J. Polym. Sci., Part A: Polym. Chem*. **2008**, *46*, 2891–2896.
(62) Urakami, H.; Guan, Z. *Biomacromolecules* **2008**, *9*, 592–597.
(63) Tang, M.; White, A. J. P.; Stevens, M. M.; Williams, C. K. *Chem. Commun*. **2009**, 941–943.
(64) Zhang, D. H.; Hillmyer, M. A.; Tolman, W. B. *Biomacromolecules* **2005**, *6*, 2091–2095.
(65) Wanamaker, C. L.; O'Leary, L. E.; Lynd, N. A.; Hillmyer, M. A.; Tolman, W. B. *Biomacromolecules* **2007**, *8*, 3634–3640.
(66) Jing, F.; Hillmyer, M. A. *J. Am. Chem. Soc*. **2008**, *130*, 13826–13827.
(67) Bueno, M.; Molina, I.; Galbis, J. A. *Carbohydr. Res*. **2009**, *344*, 2100–2104.
(68) Lowe, J. R.; Tolman, W. B.; Hillmyer, M. A. *Biomacromolecules* **2009**, *10*, 2003–2008.

(69) Wanamaker, C. L.; Bluemle, M. J.; Pitet, L. M.; O'Leary, L. E.; Tolman, W. B.; Hillmyer, M. A. *Biomacromolecules* **2009**, *10*, 2904–2911.
(70) Wanamaker, C. L.; Tolman, W. B.; Hillmyer, M. A. *Macromol. Symp.* **2009**, *283*−*84*, 130–138.
(71) Fiore, G. L.; Jing, F.; Young, V. G., Jr.; Cramer, C. J.; Hillmyer, M. A. *Polym. Chem.* **2010**, *1*, 870–877.
(72) Williams, C. K.; Breyfogle, L. E.; Choi, S. K.; Nam, W.; Young, V. G., Jr.; Hillmyer, M. A.; Tolman, W. B. *J. Am. Chem. Soc.* **2003**, *125*, 11350–11359.
(73) Kowalski, A.; Duda, A.; Penczek, S. *Macromolecules* **1998**, *31*, 2114–2122.
(74) Michinobu, T.; Bito, M.; Tanimura, M.; Katayama, Y.; Masai, E.; Nakamura, M.; Otsuka, Y.; Ohara, S.; Shigehara, K. *Polym. J.* **2009**, *41*, 843–848.
(75) Drumright, R. E.; Gruber, P. R.; Henton, D. E. *Adv. Mater.* **2000**, *12*, 1841–1846.
(76) Zhao, Y.-L.; Cai, Q.; Jiang, J.; Shuai, X.-T.; Bei, J.-Z.; Chen, C.-F.; Xi, F. *Polymer* **2002**, *43*, 5819–5825.
(77) Kazim, A.; Eren, S.; Cleva, O.-Y.; Yusuf, Z. M. *Angew. Chem., Int. Ed.* **2004**, *43*, 5210–5213.
(78) Nosonovsky, M.; Bhushan, B. In *Multiscale Dissipative Mechanisms and Hierarchical Surfaces*; Springer: Berlin, 2008; pp 81−113.
(79) Nosonovsky, M.; Bhushan, B. In *Multiscale Dissipative Mechanisms and Hierarchical Surfaces*; Springer: Berlin, 2008; pp 153−167.
(80) Nosonovsky, M.; Bhushan, B. In *Multiscale Dissipative Mechanisms and Hierarchical Surfaces*; Springer: Berlin, 2008; pp 199−230.
(81) Li, S. *J. Biomed. Mater. Res.* **1999**, *48*, 342–353.
(82) Liu, X.; Zou, Y.; Li, W.; Cao, G.; Chen, W. *Polym. Degrad. Stab.* **2006**, *91*, 3259–3265.
(83) Nerurkar, N. L.; Baker, B. M.; Sen, S.; Wible, E. E.; Elliott, D. M.; Mauck, R. L. *Nature Mater.* **2009**, *8*, 986–992.
(84) Stevens, M. M.; George, J. H. *Science* **2005**, *310*, 1135–1138.
(85) Jell, G.; Verdejo, R.; Safinia, L.; Shaffer, M. S. P.; Stevens, M. M.; Bismarck, A. *J. Mater. Chem.* **2008**, *18*, 1865–1872.